Bioorganic & Medicinal Chemistry Letters 20 (2010) 775–804

Contents lists available at ScienceDirect

Bioorganic & Medicinal Chemistry Letters

journal homepage: www.elsevier.com/locate/bmcl

Bioorganic & Medicinal Chemistry Letters Volume 20, Issue 3, 2010

Contents

ARTICLES

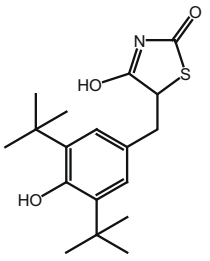

NL-1

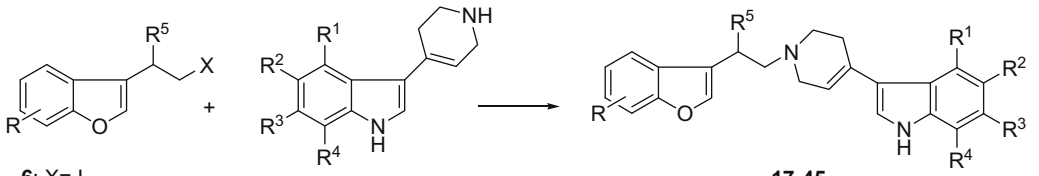

6: X= I
7: X= -OTs
R^5 is H or Me

8a-e

17-45

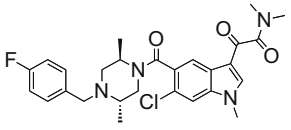

SCIO-469
p38α IC_{50} 0.009 mM

SAR studies of the p38α MAP kinase inhibitor SCIO-469 focused on maintaining activity while improving pharmacokinetic properties. Advantages were noted for compounds bearing substituents on the benzylic methylene carbon.

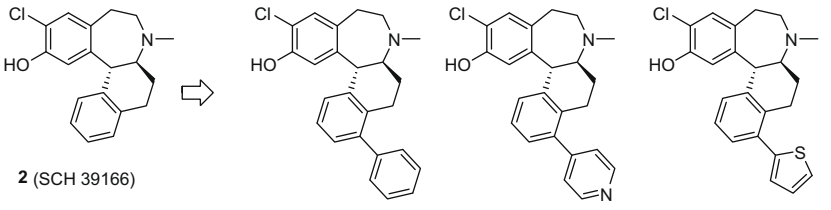

2 (SCH 39166)

8a (D_1 K_i = 0.2 nM) **8k** (D_1 K_i = 0.3 nM) **8j** (D_1 K_i = 0.9 nM)

A series of highly potent dopamine D_1 antagonists have been discovered. All compounds showed excellent selectivity over other dopaminergic receptors. Compound **8j** showed a modestly improved PK profile than SCH 39166.

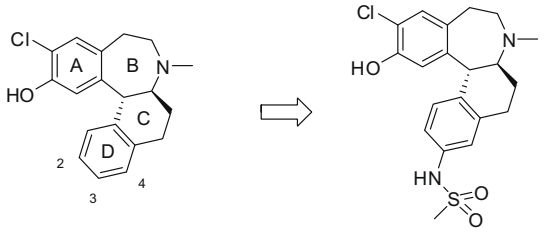

2 (SCH 39166) **17c**

The D-ring functionalization of SCH 39166 is described. Compound **17c** was discovered to have subnanomolar D_1 activity and nearly 10-fold improvement of selectivity over D_2 compared to SCH 39166. It also showed a significant improvement of PK profile.

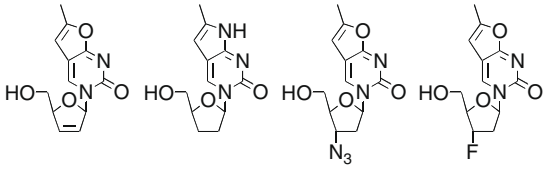

The preparation of fluorescent nucleoside analogs as molecular reporters for 2′-deoxynucleoside kinase activity is reported.

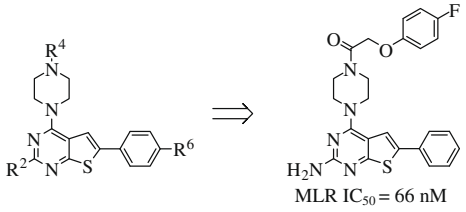

MLR IC_{50} = 66 nM

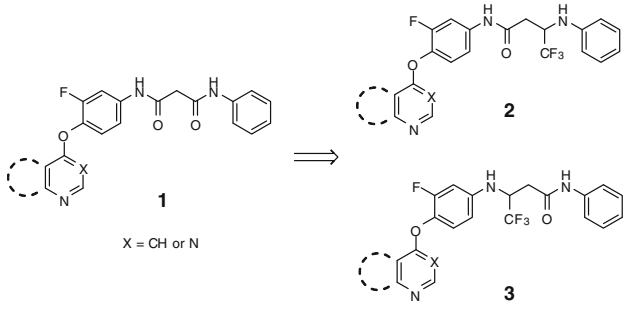

A novel series of analogues of malonamides **1**, previously known as dual c-Met/VEGFR2 inhibitors, in which one of the amide bonds was substituted by an amide isostere such as a trifluoroethylamine unit (regioisomers **2** and **3**) was prepared and evaluated for their enzymatic and cellular inhibition of VEGFR2 and c-Met enzymes. Some of these analogs (regioisomers **3**) were shown to be potent and selective inhibitors of VEGFR2 in the enzymatic assay and displayed significant effect against VEGFR-dependent angiogenic activity in cells.

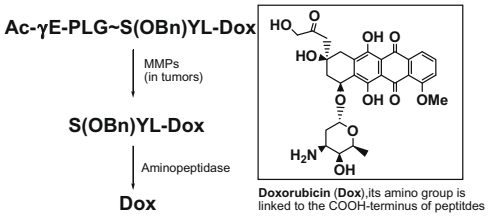

A series of MMP activated and selective peptide-doxorubicin prodrugs were discovered as efficacious antiumor agents.

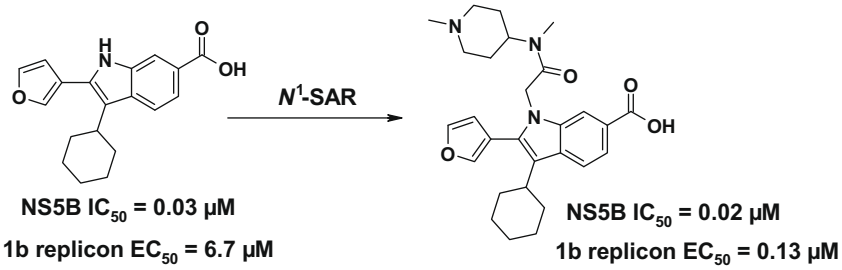

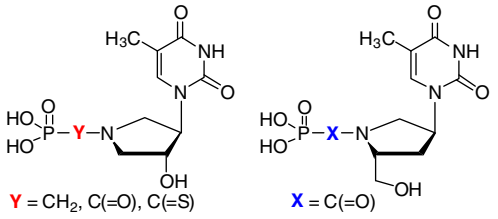

Potent inhibitors of the rat T-cell lymphoma thymidine phosphorylase with IC_{50} values within 11–45 nM.

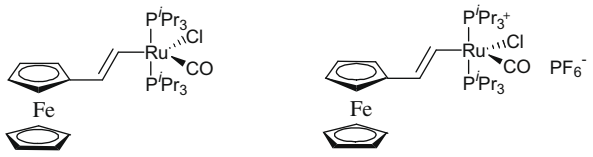

Mixed ferrocene/ruthenium bioorganometallics.

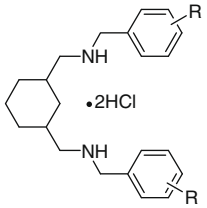

21 Examples

	MIC (μg/mL)			
R-4	*E. coli*	*P. aeruginosa*	*S. aureus*	*S. epidermidis*
Et	NA	0.125	NA	0.25
n-Pr	0.016	0.016	NA	0.016
n-Bu	0.016	0.002	0.004	0.004
t-Bu	0.002	0.004	0.016	0.008

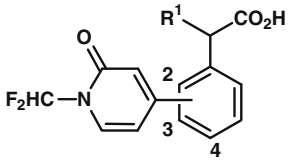

2-, 3- and 4-regioisomers
R^1 = H, Me

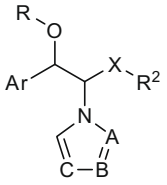

The development of novel small molecule inhibitors of PAR1 is described.

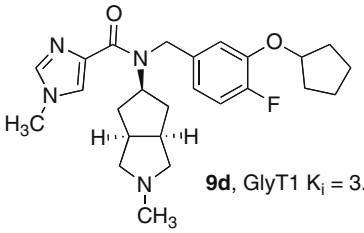

9d, GlyT1 K_i = 3.76 nM

The discovery of a potent, selective inhibitor of the type 1 glycine transporter, **9d**, is reported.

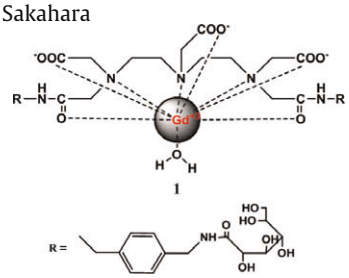

A new type of dendritic molecule Gd-DTPA-XDA-D1-Glc(OH), whose ligand worked to coordinate gadolinium(III) ion at the center of their frameworks with two glucose moieties on the molecular surfaces, was readily synthesized with high yield. The structure was established by IR, ^{1}H, ^{13}C NMR, and mass spectral studies. Its bio-distribution patterns were evaluated on rats.

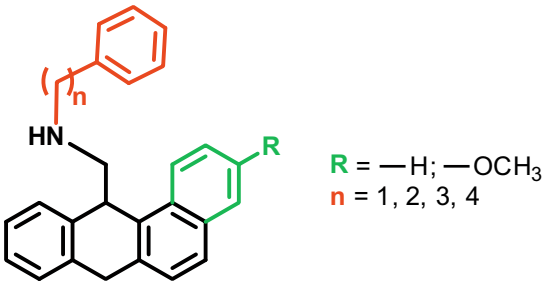

The synthesis, biological evaluation, and molecular modeling of dihydrotetracene/dihydrotetraphene and *N*-phenylalkyl analogs of AMDA as molecular probes of the ligand binding sites in 5-HT_{2A} and H_1 receptors is reported.

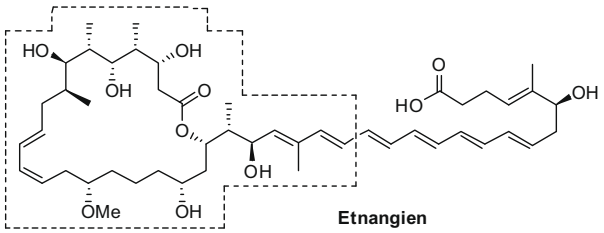

Novel simplified analogues of the potent RNA polymerase inhibitor etnangien were obtained by total synthesis and evaluated for antibacterial activity against Gram-positive bacteria and one Gram-negative bacterium.

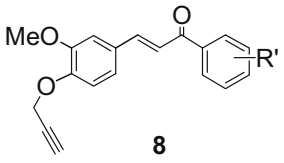

The synthesis and evaluation of a series of acetylenic chalcones as antimalarial and antitubercular agents is described.

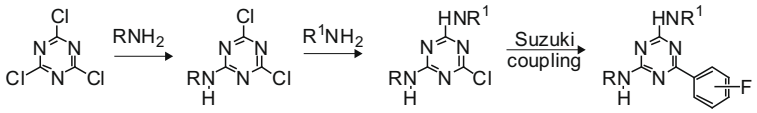

A number of low molecular weight fluorophenyl triazine molecules that show antimicrobial activity.

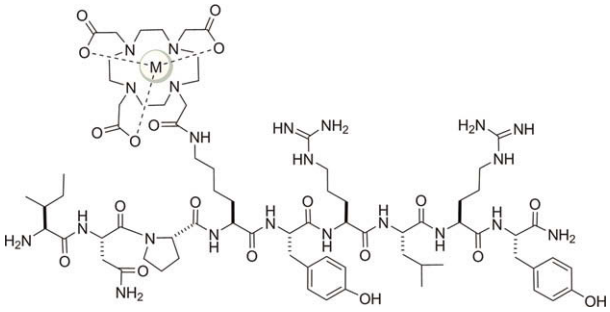

[Lys(DOTA)^4]BVD15, a potent NPY Y_1 analog suitable for radiolabeling with metallo positron emitters for PET imaging of breast cancer.

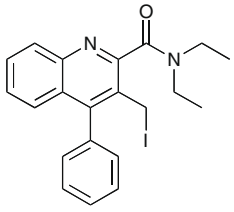

K_i= 12.0 nM

A new library of iodinated quinoline-2-carboxamides has been prepared and tested for affinity with the translocator protein (TSPO). *N*,*N*-Diethyl-3-iodomethyl-4-phenylquinoline-2-carboxamide was found to have excellent affinity with a K_i value of 12.0 nM.

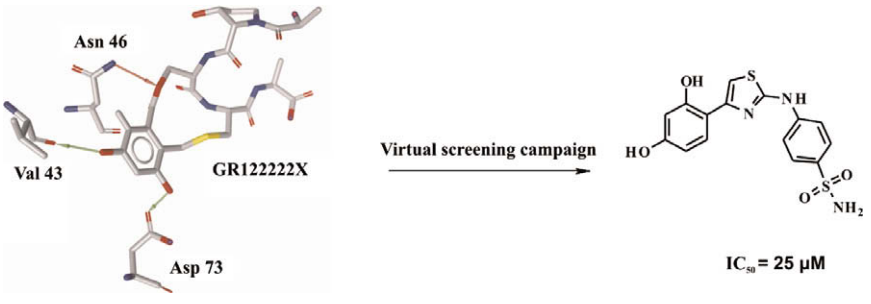

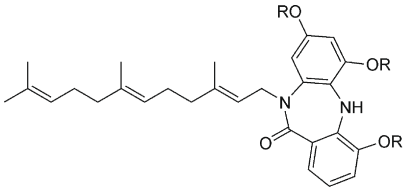

1 (BU-4664L): R=H
3: R=Me

BU-4664L (**1**) was found to inhibit tumor cell invasion and angiogenesis by interrupting cellular motility. Compound **3** displayed the highest in vitro anti-angiogenic effect (IC_{50} = 0.22 μM).

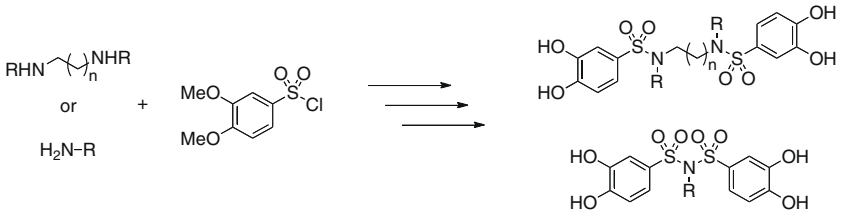

The synthesis and evaluation of potent and novel bis-arylsulfonamide and arylsulfonimide-based inhibitors of plasminogen activator inhibitor-1 (PAI-1) is described.

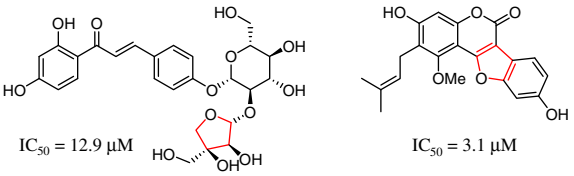

The efficacy of the neuraminidase inhibition appears to be relatively to present of five-membered ring in polyphenols.

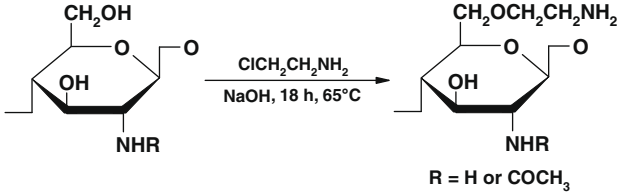

Two kinds of aminoethyl-chtiosans (AEC), AEC90 and AEC50, having degrees of deacetylation of 90% and 50%, exhibited strong synergistic effects in combination with β-lactams against MRSA.

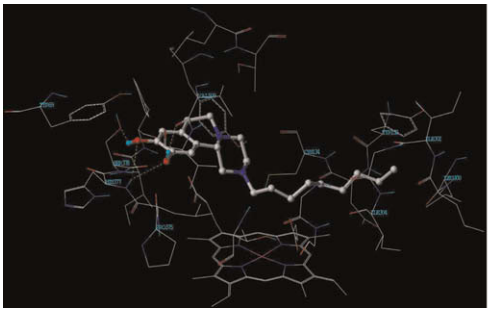

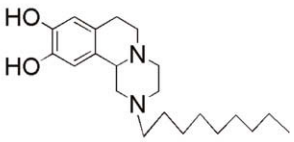

The mode of action of compound **13a** with the active site of CYP51 of *Candida albicans* is reported.

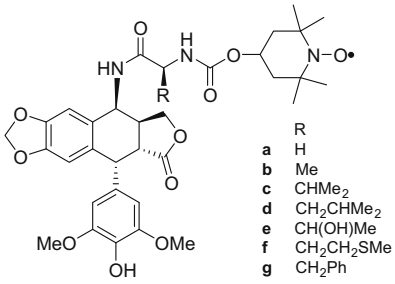

	R
a	H
b	Me
c	$CHMe_2$
d	CH_2CHMe_2
e	CH(OH)Me
f	CH_2CH_2SMe
g	CH_2Ph

The synthesized compounds showed superior or comparable cytotoxicities and pronounced antioxidative activity compared to VP-16.

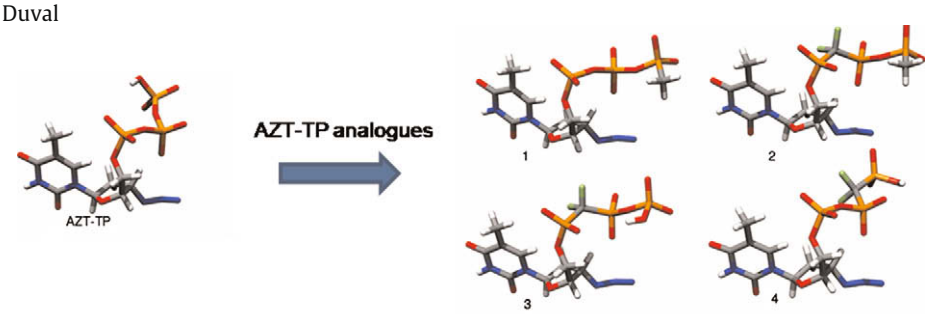

This Letter describes the design of stable triphosphate analogues of AZT using molecular modelling, their synthesis and their use for producing anti AZT-TP antibodies for developing an immunoassay for TDM.

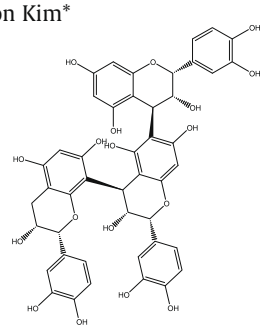

Compound **3** showed collagenase, gelatinases A and B inhibitory activity (IC_{50}) at 0.34, 0.4 and 2.3 μM, respectively. The presence of an epicatechin-(4β→6) moiety may play an important role in collagenase and gelatinase inhibitory activities.

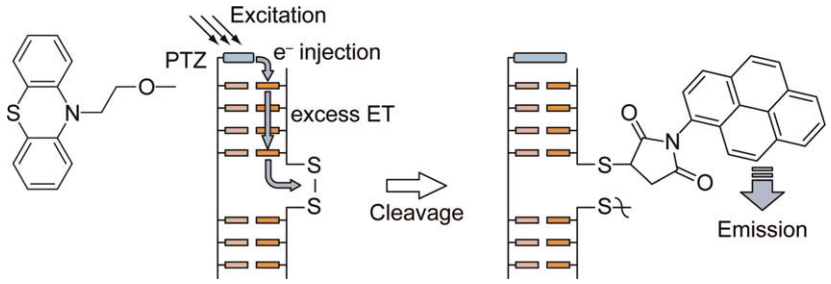

A new method for fluorescence analysis of excess electron transfer through DNA based on reductive cleavage of a disulfide bond and a thiol-specific fluorescent probe is described.

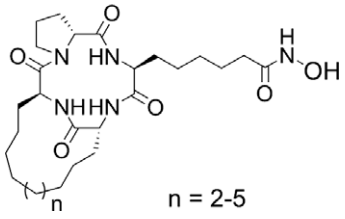

A series of bicyclic tetrapeptide hydroxamic acids were designed and synthesized as histone deacetylase (HDAC) inhibitors. Most of them were found to be potent inhibitors with remarkable selectivity among the HDACs. The in vivo activity depends on alkyl loop length.

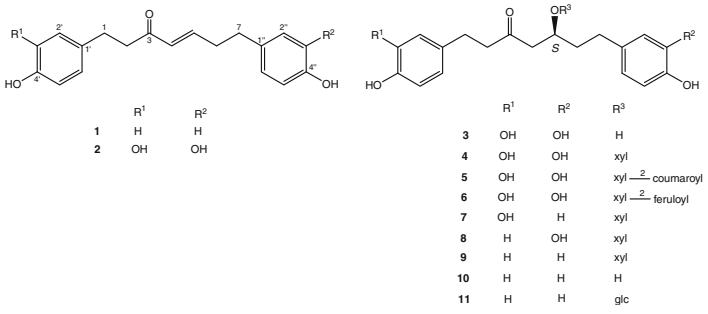

	R^1	R^2	R^3
1	H	H	
2	OH	OH	
3	OH	OH	H
4	OH	OH	xyl
5	OH	OH	xyl—2—coumaroyl
6	OH	OH	xyl—2—feruloyl
7	OH	H	xyl
8	H	OH	xyl
9	H	H	xyl
10	H	H	H
11	H	H	glc

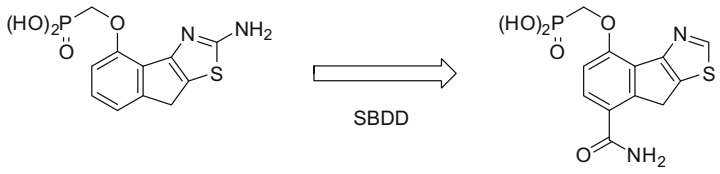

6

FBPase IC_{50} = 124 nM

19a

FBPase IC_{50} = 1 nM

Our structure-based drug design efforts led to the finding of **19a** as potent FBPase inhibitor (FBPase IC_{50} = 1 nM).

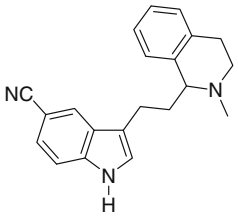

(–)-21a
hSERT IC_{50} = 0.42 nM

A series of ring constrained homotryptamine analogs was prepared in 5 steps from 1-tosyl-3-vinylindoles via [3+2] dipolar cycloaddition with cyclic nitrones. The final products, including **(–)-21a**, demonstrated potent and selective binding affinity for the human serotonin transporter (hSERT).

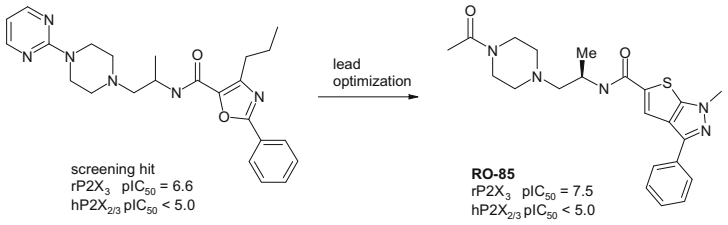

The discovery and optimization of RO-85, a novel drug-like, potent and selective $P2X_3$ antagonist is described.

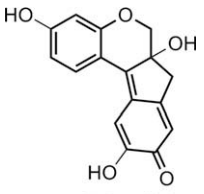

1, Brazilein

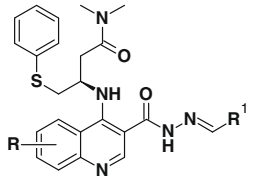

(13a-m, 14a-m)

R = 8-CF_3, 6-F
R^1 = Aromatic/aliphatic group

Synthesis of a new series of quinoline-3-carbohydrazones is presented together with the pharmacological profiles. Compounds **13e**, **13i**, **13k**, **14a**, **14c**, and **14i** emerged as the lead molecules with **MIC** ranging 0.625–5 μg/mL and did not show toxicity on Vero cells up to 62.5 μg/mL which are in comparable with the present first line anti tuberculosis drugs.

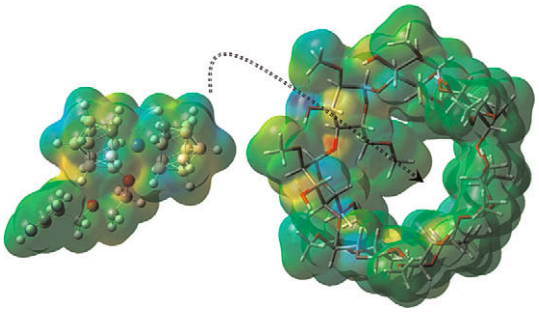

Scheme of cobalt bis(dicarbollide) derivative **2** and DIMEB.

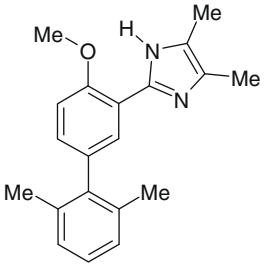

(4b)

We report the identification of a novel biaryl template for H^+/K^+ ATPase inhibition. Evaluation of critical SAR features within the biaryl imidazole framework and the use of pharmacophore modelling against known imidazopyridine and azaindole templates suggested that the geometry of the molecule is key to achieving activity. Herein we present our work optimising the potency of the molecule through modifications and substitutions to each of the ring systems. In particular sub-micromolar potency is achieved with (**4b**) presumably through a proposed intramolecular hydrogen bond that ensures the required imidazole basic centre is appropriately located.

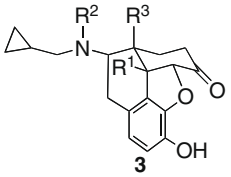

3

Novel 16,17-*seco*-naltrexone derivatives **3** were synthesized using 16–17 bond cleavage reaction of naltrexone as the key reaction to examine the Beckett–Casy model.

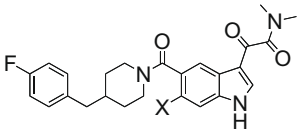

1, X = Cl, p38α IC_{50} 0.018 μM
2, X = OMe, p38α IC_{50} 0.01 μM

A new class of p38α MAP kinase inhibitors based on 4-fluorobenzylpiperidine substituted heterocycles is described. Optimal features include a piperidine and an oxalyl amide separated by a [6,5] fused ring heterocycle.

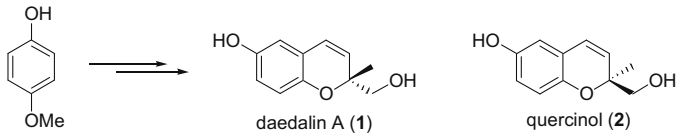

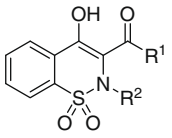

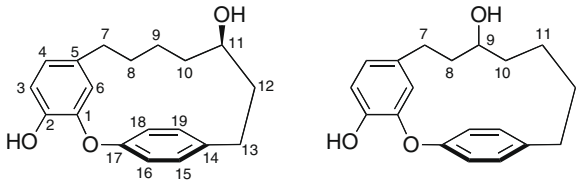

Two cyclic diarylheptanoids, acerogenins A (**1**) and B (**2**) have been isolated from the bark of *Acer nikoense* as inhibitors of Na^+-glucose cotransporter (SGLT). Acerogenins A (**1**) and B (**2**) inhibited both isoforms, SGLT1 and SGLT2. Structure–activity relationship of acerogenin derivatives on inhibitory activity of SGLT as well as conformational analysis of **1** and **2** on the basis of *J*-resolved HMBC spectra and X-ray analysis were discussed.

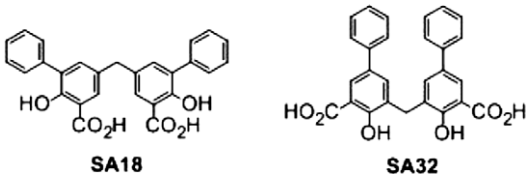

SA18 and **SA32** inhibited IKK-β both in vitro and in vivo suggesting a novel mechanism of the anti-obesity effect by these compounds.

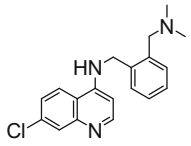

The synthesis and in vivo efficacy of phenylequine salts is reported (ED_{50} of 0.81 in *Plasmodium yoelii*).

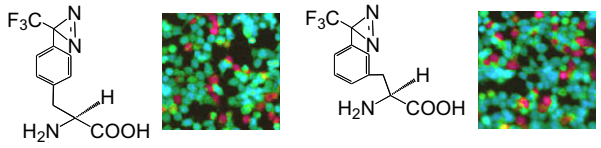

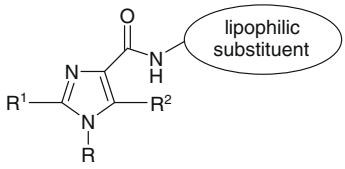

Imidazoles represent a novel chemotype of potent and selective CB_2 receptor antagonists.

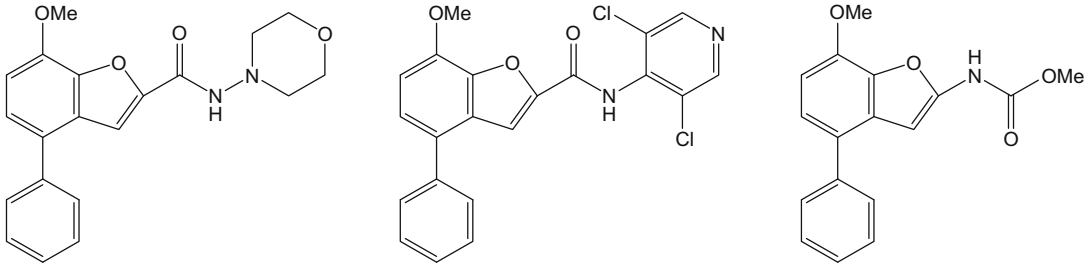

Novel benzofuran derivatives as potent and selective adenosine A_{2A} inhibitors were synthesized and evaluated.

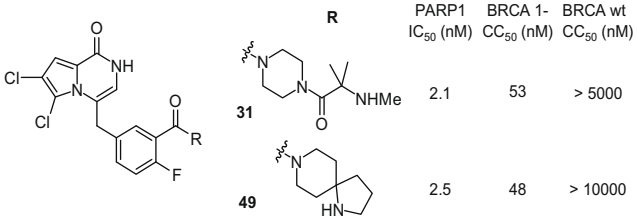

The discovery and optimization of a novel series of pyrrolo[1,2-*a*]pyrazin-1(2*H*)-one PARP inhibitors is reported, leading to potent inhibitors displaying excellent anti-proliferation activity in BRCA deficient cells.

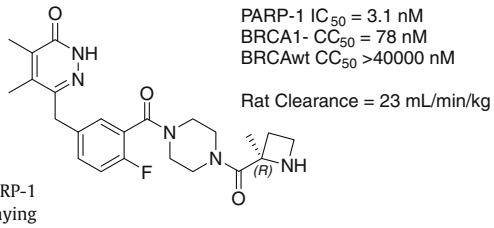

An extensive SAR exploration of the dimethylpyridazin-3(*2H*)-one scaffold led to the identification of potent PARP-1 inhibitors, capable of inhibiting the proliferation of BRCA-1 deficient cancer cells in the low nanomolar range, displaying >100-fold selectivity over the BRCA proficient cells, with clean off-target profiles and low clearance in rats.

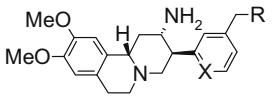

R = F, X = CH; IC_{50} = 0.5 nM
R = H, X = N; IC_{50} = 19 nM

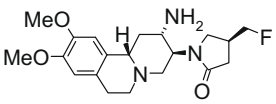

carmegliptin (**8p**)

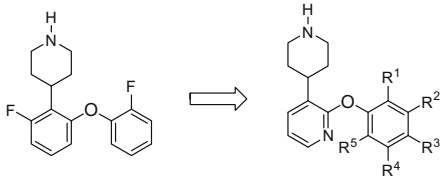

A conformational analysis of 4-phenylpiperazine (left) and 4-phenyl-1,2,3,6-tetrahydropyridine (right) derivatives demonstrates that the privileged almost planar orientation of the 4-substituted phenyl ring found in the latter is more favourable for 5-HT$_{1A}$ affinity.

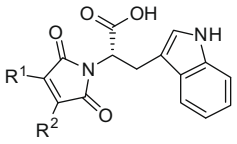

5: R^1 = R^2 = H
6: R^1 = H, R^2 = CH$_3$
7: R^1 = H, R^2 = Ph
8: R^1 = CH$_3$, R^2 = CH$_3$

To identify novel non-nucleoside DNA methyltransferase (DNMT) inhibitors, we designed and synthesized a series of maleimide derivatives. Among this series, compounds **5–8** were found to be more potent DNMT1 inhibitors than RG108, a DNMT1 inhibitor reported previously by Siedlecki et al.

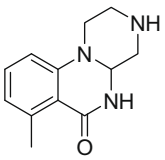

Compound (+)-**2a**
5-HT$_{2C}$ EC$_{50}$ 45 nM (IA = 1)
5-HT$_{2B}$ EC$_{50}$ >10000 nM (IA = 0)
5-HT$_{2A}$ EC$_{50}$ >10000 nM (IA = 0)

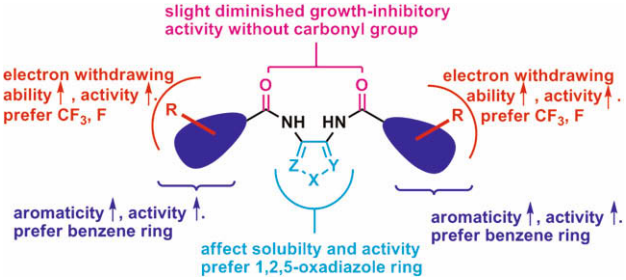

Schematic representation of structure–activity relationships based on diverse furazan-3,4-diamide analogs.

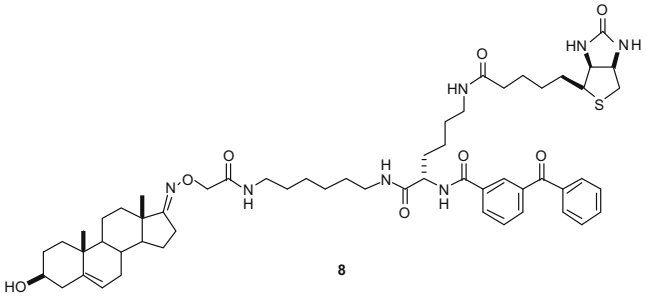

8

A novel analog of DHEA, carrying both benzophenone and biotin groups, retains the biological activity of DHEA and can be used for analysis and isolation of cellular DHEA binding sites.

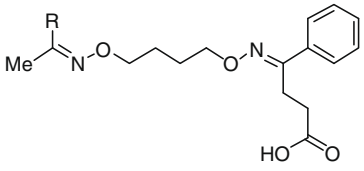

9d, R=4-methoxyphenyl
9m, R=3-methoxy-4-methylphenyl

A novel class of selective PPARα agonists containing bis-oximinoalkanoic acid was described. Selected compounds **9d** and **9m** showed excellent potency and high selectivity towards PPARα in vitro and found to be effective in reducing serum triglycerides (TG) in vivo.

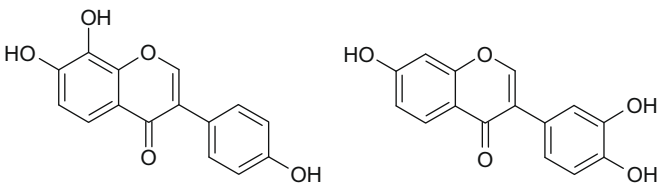

1 **2**

Natural melanin formation inhibitors from aged Korean fermented soybean paste (**1**–**2**) are reported.

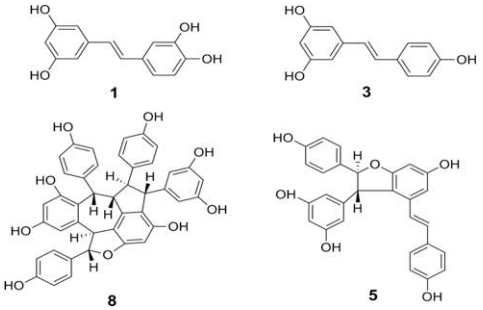

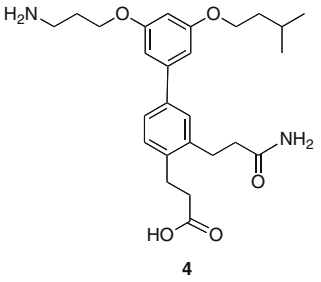

The synthesis of ligand **4** binds to G-CSF receptor is reported.

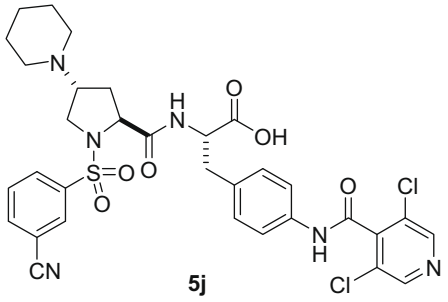

Compounds such as **5j** (IC_{50} = 0.11 nM) are potent inhibitors of VLA-4.

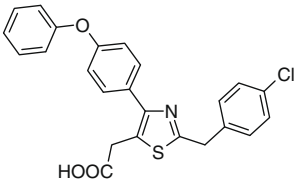

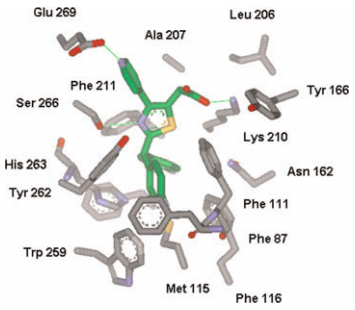

SAR has been established by exploring the eastern and western side of 5-thiazoleacetic acids supported by modeling and docking studies.

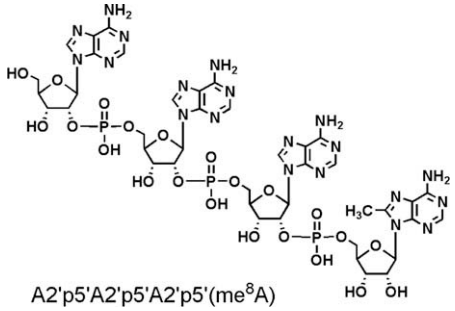

The 5′-phosphoryl group of 2-5A is reportedly necessary for the conformational change leading to RNase L activation. However, we found that 5′-*O*-dephosphorylated 2-5A tetramer analogs with 8-methyladenosine at the 2′-terminus were more effective as an activator of RNase L than the parent 2-5A tetramer. Introduction of 8-methyladenosine is thought to induce a dramatic shift of 2-5A in the binding site of RNase L.

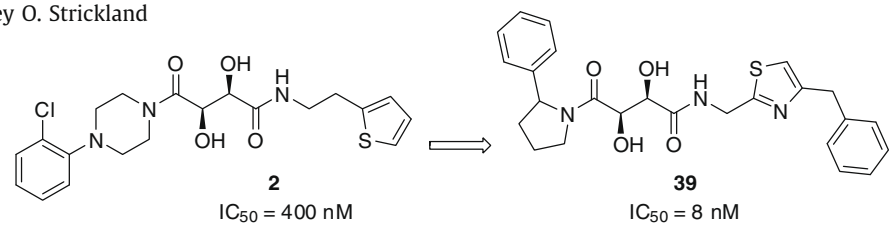

Synthesis and optimization of novel tartrate TACE inhibitors are described.

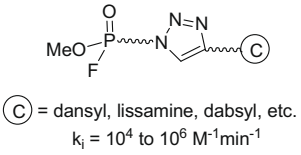

The synthesis and inhibition of AChE by a series of chromophore-linked fluorophosphonates is reported.

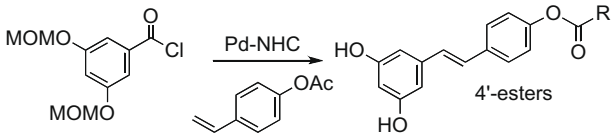

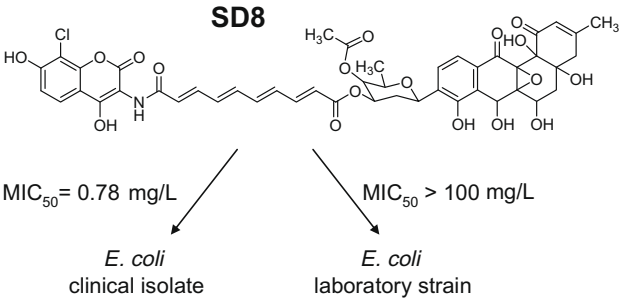

The lipocalin protein plasma drug transporter α -acid glycoprotein possesses chaperone-like activity evidenced by suppressing heat- and chemical-induced aggregation of various proteins.

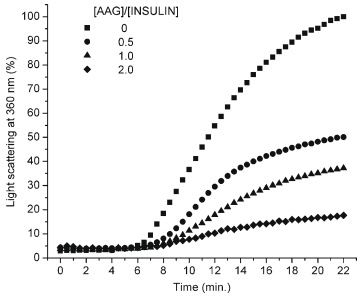

1

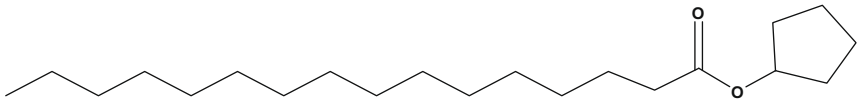

13

N-Acylethanolamine-hydrolyzing acid amidase (NAAA) specifically hydrolyzes *N*-palmitoylethanolamine, an anti-inflammatory mediator. We synthesized and screened several new compounds, and *cyclopentylhexadecanoate* (**13**) exhibited the highest inhibitory activity on NAAA.

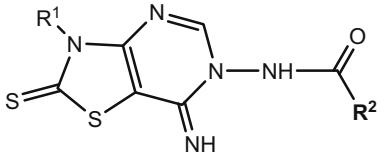

16, R^1 = -C_3H_7; R^2 = NH_2

Novel bicyclic thiazolopyrimidine compounds (**15**–**26**) were synthesized and their in vitro binding studies and functional assay (cAMP determination) showed that compound (**16**) is a potent and selective A_{2A}R antagonist with strong binding affinity (K_i value = 0.0038 nM) towards A_{2A}R and higher selectivity (737-fold) versus A_1R.

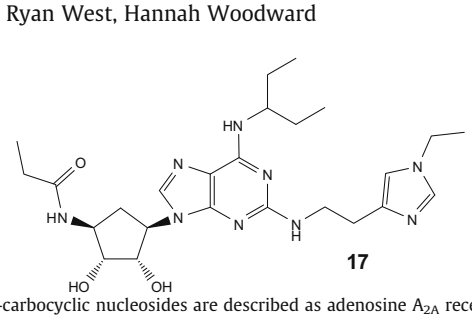

17

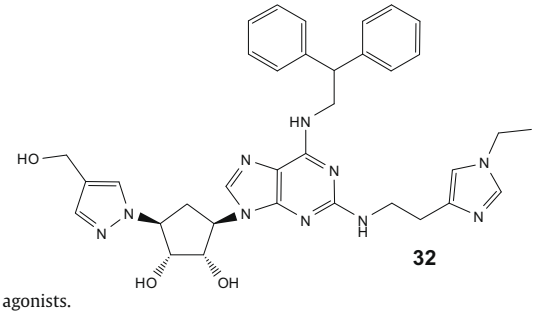

32

Two series of 4′-aza-carbocyclic nucleosides are described as adenosine A_{2A} receptor agonists.

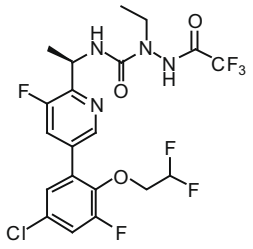

4k

Benzamides and semicarbazides are introduced as new classes of bradykinin B_1 receptor antagonists. The best compounds feature excellent pharmacokinetic properties in the rat.

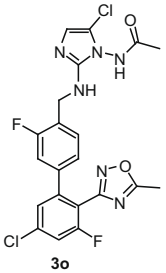

3o

New bradykinin B1 receptor antagonists based on 5-membered diaminoheterocycles with nanomolar activity are presented.

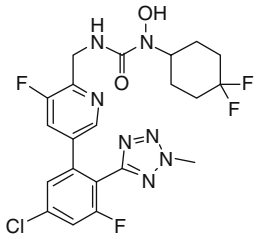

2o

Hydroxy urea analogues have been developed as a new class of bradykinin B1 receptor antagonists. Systematic optimization led to the identification of several antagonists with low-nanomolar activity and very high oral bioavailability in the rat.

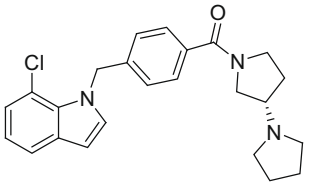

Using a focused screen of biogenic amine compounds a novel series of H_3R antagonists was identified. Preliminary SAR led to reduction of MW while increasing binding affinity and potency. Optimization of the physical properties of the series led to (*S*)-**6n**, with improved brain to plasma exposure and efficacy in both water intake and novel object recognition models.

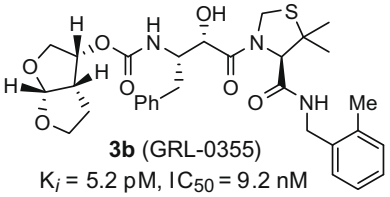

3b (GRL-0355)

K_i = 5.2 pM, IC_{50} = 9.2 nM

A series of novel HIV-1 protease inhibitors were designed and synthesized incorporating stereochemically defined and conformationally constrained cyclic ethers as P2-ligands into allophenylnorstatine based isostere. Inhibitor **3b** with a bis-THF P2-ligand has shown impressive potency.

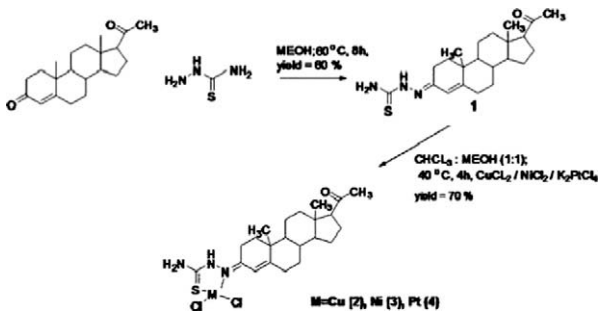

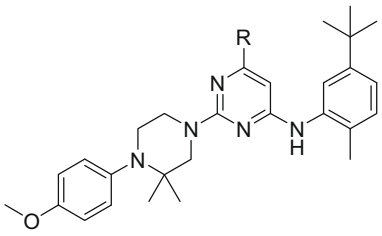

The development of a novel series of piperazinyl pyrimidines as γ-secretase modulators for potential use in the treatment of Alzheimer's disease is disclosed herein. Optimization of a screening hit provided a series of potent γ-secretase modulators with >180-fold in vitro selectivity over inhibition of Notch cleavage.

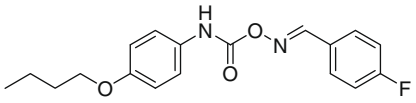

50 IC_{50} = 2.2±0.9 nM

The rationale behind the discovery and the biological evaluations of this novel class of FAAH inhibitors are presented. Both in vitro and in vivo results of selected targets are discussed, along with inhibition kinetics and molecular modeling studies.

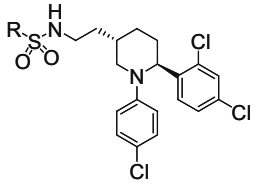

hCB_1 K_i = 3-61 nM

A series of mono- and di-substituted *N*-arylaminomethylene malonates have been used to probe the potential of utilizing additional H-bonding contacts in the ubiquinone binding channel, for selective inhibition between either human or *Plasmodium* DHODH. The resulting trends in measured affinity were rationalized using molecular docking.

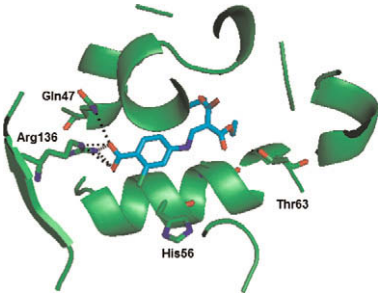

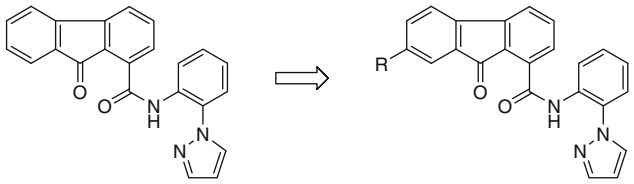

The synthesis and SAR of a group of apoptosis inducing 9-oxo-9*H*-fluorene-1-carboxamides with modifications at the 9-oxo-9*H*-fluorene ring are reported.

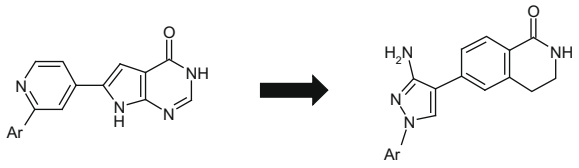

3-Aminopyrazole based MK2-inhibitors were discovered by scaffold hopping strategy. Optimized derivatives proved to inhibit intracellular phosphorylation of hsp27 as well as LPS-induced TNFα release in cells and in vivo.

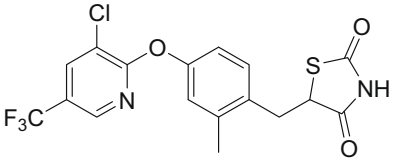

Systematic structure–activity relationship (SAR) studies of a screening lead led to the discovery of a series of thiazolidinediones (TZDs) as potent GPR40 agonists. Among them, compound **C** demonstrated an acute mechanism-based glucose-lowering in an intraperitoneal glucose tolerance test (IPGTT) in lean mice, while no effects were observed in GPR40 knock-out mice.

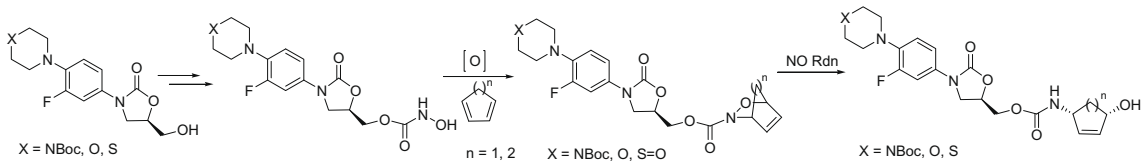

A series of novel oxazolidinone antibiotics having [2,2,1] and [2,2,2] bicyclic oxazine moieties at the C-5 side chain of the A-ring were synthesized by nitroso Diels–Alder reactions, from three linezolid analogs containing morpholine, piperazine and thiomorpholine, respectively, as the C-ring components. Subsequent N–O bond cleavage generated oxazolidinones with 4-amino cycloalk-2-en-1-ol substituents. The in vitro antibacterial activities of these oxazolidinone analogs were evaluated.

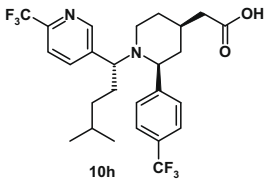

Compound **10h** was found to be a potent modulator in vitro and was found to decrease Aβ42, increase Aβ38 and have no effect on Aβ40 levels. Furthermore, **10h** demonstrated excellent pharmacokinetic parameters in the mouse, rat and dog in addition to good CNS penetration in the mouse.

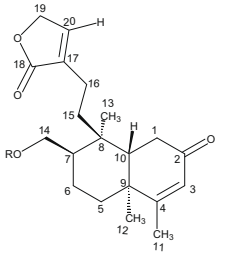

Gomphostenin **1** R = H
Gomphostenin-A **2** R = $COCH_3$

Phytochemical investigation of $CHCl_3$ extract of the *Gomphostemma niveum* leaves led to the isolation of two new diterpene, compound **1** and **2**. Their structures were elucidated by spectroscopic procedures and single crystal XRD. Compound **1** named as Gomphostenin **1** and structure was established as 8-ethyl (5*H*-furan-2-one, 14-hydroxy, 2-oxo 3, 20 *Z*(*17*) diene clerodane, while compound **2** named as Gomphostenin-A was found to be the acetyl derivative of compound **1** and revealed as 8-ethyl (5*H*-furan-2-one, 14-acetoxy, 2-oxo 3, 20 *Z*(*17*) diene clerodane **.** In vitro antimalarial activity against *Plasmodium falciparum* showed that compound **2** was more active than compound **1** and $CHCl_3$ extract as well; with IC_{50} value of 3.4 μg/mL

*Corresponding author
Supplementary data available via ScienceDirect

COVER

Overlay of high resolution co-crystal structures of *R*-**22**-ADP (cyan) and **1**-ADP (green) bound in an allosteric binding site of the mitotic kinesin KSP. [Roecker, A. J.; Coleman, P. J.; Mercer, S. P.; Schreier, J. D.; Buser, C. A.; Walsh, E. S.; Hamilton, K.; Lobell, R. B.; Tao, W.; Diehl, R. E.; South, V. J.; Davide, J. P.; Kohl, N. E.; Yan, Y.; Kuo, L. C.; Li, C.; Fernandez-Metzler, C.; Mahan, E. A.; Prueksaritanont, T.; Hartman, G. D. *Bioorg. Med. Chem. Lett.* **2007**, *17*, 5677.]

Indexed/Abstracted in: Beilstein, Biochemistry & Biophysics Citation Index, CANCERLIT, Chemical Abstracts, Chemistry Citation Index, Current Awareness in Biological Sciences/BIOBASE, Current Contents: Life Sciences, EMBASE/Excerpta Medica, MEDLINE, PASCAL, Research Alert, Science Citation Index, SciSearch, TOXFILE. Also covered in the abstract and citation database SCOPUS®. Full text available on ScienceDirect®

ELSEVIER

ISSN 0960-894X